

# Parametric Studies of Ultrarelativistic Electron Acceleration by an Oblique Shock Wave<sup>\*)</sup>

Mieko TOIDA and Junya INAGAKI

*Department of Physics, Nagoya University, Nagoya 464-8602, Japan*

(Received 26 November 2013 / Accepted 11 February 2014)

A magnetosonic shock wave propagating obliquely to an external magnetic field can trap and accelerate electrons to ultrarelativistic energies when  $v_{\text{sh}}$  is close to  $c \cos \theta$ , where  $v_{\text{sh}}$  is the propagation speed of the shock wave,  $c$  is the light speed, and  $\theta$  is the propagation angle of the shock wave. Because of instabilities driven by the trapped electrons, some electrons can be detrapped from the main pulse retaining their high energies and can then be further accelerated to higher energies as a result of their gyromotions. The dependence of electron motions on the parameters  $v_{\text{sh}}$  and  $\theta$  is investigated by two-dimensional electromagnetic particle simulations with full ion and electron dynamics. If  $\theta$  is fixed, electron energies become maximum when  $v_{\text{sh}}$  is slightly smaller than  $c \cos \theta$ . If the value of  $v_{\text{sh}}/(c \cos \theta)$  is fixed, the maximum energy of electrons tends to increase with decreasing  $\theta$  for the range  $v_{\text{sh}}/(c \cos \theta) < 1$ . The number of electrons that are detrapped to the upstream region and suffer the subsequent acceleration is also examined.

© 2014 The Japan Society of Plasma Science and Nuclear Fusion Research

Keywords: particle acceleration, collisionless shock, trapping, detrapping, particle simulation

DOI: 10.1585/pfr.9.3401026

## 1. Introduction

Particle simulations have revealed [1] that prompt electron acceleration to ultrarelativistic energies can occur in a magnetosonic shock wave propagating obliquely to an external magnetic field with a propagation speed  $v_{\text{sh}}$  close to  $c \cos \theta$ , where  $c$  is the light speed and  $\theta$  is the propagation angle of the shock wave. In such a wave, some electrons can be reflected near the end of the main pulse of the shock wave. (If the damping is small, the shock wave approximates a train of solitons. We call the first leading pulse, the main pulse.) Then, the reflected electrons become trapped and are energized in the main pulse region. The energies of accelerated electrons increase as the external magnetic field becomes stronger.

Recently, it has been shown that multi-dimensional effects can significantly influence electron motions in an oblique shock wave [2, 3]. One-dimensional (1D) simulations demonstrated that once electrons become trapped in the main pulse, they cannot readily escape from the wave [4]. However, two-dimensional (2D) simulations showed that after trapping and energization in the main pulse, some electrons can be detrapped from the main pulse, retaining their ultrarelativistic energies. Further, the electrons detrapped to the upstream region can be accelerated to much higher energies by the mechanism reported in Ref. [5] for accelerating fast ions. The detrapping is caused by 2D electromagnetic fluctuations along the shock front excited by trapped electrons [2].

author's e-mail: toida@cc.nagoya-u.ac.jp

<sup>\*)</sup> This article is based on the presentation at the 23rd International Toki Conference (ITC23).

The above 2D simulations were performed for the case in which  $v_{\text{sh}} \simeq 0.95c \cos \theta$  and the Alfvén Mach number  $M_A = 2.3$ . In this paper, we study how the motions in an oblique shock wave depend on the parameters  $v_{\text{sh}}$  and  $\theta$  using a 2D relativistic electromagnetic particle code with full ion and electron dynamics.

## 2. Electron Motion in an Oblique Shock Wave

We present some theoretical expressions for electron motions in an oblique shock wave. We assume that a shock wave propagates in the  $x$ -direction with a constant speed  $v_{\text{sh}}$  in an external magnetic field in the  $(x, z)$  plane,  $\mathbf{B}_0 = B_0(\cos \theta, 0, \sin \theta)$ . Assuming that the shock wave is 1D and stationary, we can write the maximum Lorentz factor of electrons trapped in the main pulse as [6]

$$\gamma_m \sim \frac{\Omega_e^2}{\omega_{\text{pe}}^2} \frac{v_{\text{sh}} c \cos \theta}{v_A (c \cos \theta - v_{\text{sh}})} = \frac{\Omega_e^2}{\omega_{\text{pe}}^2} \frac{c \langle v_{\text{sh}} \rangle \cos \theta}{v_A (1 - \langle v_{\text{sh}} \rangle)}, \quad (1)$$

where  $\Omega_e (< 0)$  and  $\omega_{\text{pe}}$  are the electron gyro frequency and plasma frequency, respectively, in the upstream region, and  $\langle v_{\text{sh}} \rangle$  is defined by

$$\langle v_{\text{sh}} \rangle = v_{\text{sh}} / (c \cos \theta). \quad (2)$$

The theory (1) was derived under the condition that  $\langle v_{\text{sh}} \rangle$  is smaller than unity. This theory is in good agreement with 1D simulation results [6].

The theoretical analysis also showed that relative velocity between the guiding center of the trapped electrons

and the shock wave can be written as [6]

$$v_x = (c \cos \theta - v_{\text{sh}})B_0/B. \quad (3)$$

This indicates that electrons cannot readily escape from the main pulse when  $v_{\text{sh}} \approx c \cos \theta$  because  $v_x \approx 0$ .

Equation (3) was extended to include 2D and nonstationary effects as [7]

$$v_x \approx (c \cos \theta - v_{\text{sh}} + c\delta f_{11} + c\delta f_{12})B_0/B, \quad (4)$$

with

$$\delta f_{11} \approx \delta E_{y1}/B_0, \quad \delta f_{12} \approx (\delta B_{x2} + \delta E_{y2})/B_0. \quad (5)$$

Here,  $\delta f_{12}$  is due to 2D fluctuations of electromagnetic fields defined as

$$\delta E_2(x, y, t) = \mathbf{E}(x, y, t) - \bar{\mathbf{E}}(x, t), \quad (6)$$

$$\delta B_2(x, y, t) = \mathbf{B}(x, y, t) - \bar{\mathbf{B}}(x, t), \quad (7)$$

where  $\bar{\mathbf{E}}$  and  $\bar{\mathbf{B}}$  are  $\mathbf{E}$  and  $\mathbf{B}$  averaged along the  $y$ -direction. We call  $\bar{\mathbf{E}}$  and  $\bar{\mathbf{B}}$  1D fields. Nonstationarity of the 1D field produces  $\delta f_{11}$ . When the shock wave is 1D and stationary ( $\delta f_{11} = \delta f_{12} = 0$ ), Eq. (4) reduces to Eq. (3). If the magnitudes of  $\delta f_{11}$  and  $\delta f_{12}$  are not small,  $v_x \approx 0$  can break down even when  $v_{\text{sh}} \approx c \cos \theta$ . This indicates that some electrons can be detrapped from the main pulse under the influence of the fluctuations  $\delta f_{11}$  and  $\delta f_{12}$ .

Electrons detrapped to the upstream region can reenter the shock wave because of their gyromotions if the electron gyroradii are large enough. Then, they are accelerated to higher energies by the mechanism discussed in Ref. [5] for fast ions. That is, the electrons are accelerated by the transverse electric field  $E_y$  in the shock wave because the gyromotions are antiparallel to  $E_y$ . The energy increases once in the gyroperiod; the increment of  $\gamma$  is theoretically given by [5]

$$\delta\gamma \sim \alpha v_{\perp} \gamma, \quad (8)$$

where  $\alpha$  is a constant.

### 3. Simulation Method and Parameters

We use a 2D (two spatial coordinates and three velocity components) relativistic electromagnetic particle code with full ion and electron dynamics. The system size is  $L_x \times L_y = 16384\Delta_g \times 512\Delta_g$ , where  $\Delta_g$  is the grid spacing. The total number of simulation particles is  $N \approx 1.1 \times 10^9$ . We follow the orbits of  $2.1 \times 10^6$  electrons, which we call 2Ds electrons. For comparison, we calculate test particle motions in the 1D fields,  $\bar{\mathbf{E}}(x, t)$  and  $\bar{\mathbf{B}}(x, t)$ , obtained in the 2D simulation. We denote these test electrons as 1Dt electrons. The number of 1Dt electrons is the same as that of 2Ds electrons. The initial positions and velocities of the 1Dt electrons are exactly the same as those of the 2Ds electrons.

The ion-to-electron mass ratio is  $m_i/m_e = 400$ ; although the real value of  $m_i/m_e (\approx 1836)$  is desirable, we chose a smaller one because of limited computer power. The speed of light is  $c/(\omega_{pe}\Delta_g) = 4.0$ , and the electron and ion thermal velocities in the upstream region are  $v_{Te}/(\omega_{pe}\Delta_g) = 0.5$  and  $v_{Ti}/(\omega_{pe}\Delta_g) = 0.025$ , respectively. The external magnetic field in the  $(x, z)$  plane is  $\mathbf{B}_0 = B_0(\cos \theta, 0, \sin \theta)$ , and its strength is  $|\Omega_e|/\omega_{pe} = 5$  in the upstream region.

In Ref. 3, the results for  $\theta = 54^\circ$ ,  $v_{\text{sh}} = 0.95c \cos \theta$ , and  $M_A = 2.3$  were presented. In this study, we perform simulations for various values of  $v_{\text{sh}}$  and  $\theta$  and study the parametric dependence of electron motions.

### 4. $v_{\text{sh}}$ Dependence

We firstly present the results for  $\theta = 54^\circ$  and  $v_{\text{sh}} = 0.90c \cos \theta$ . Figure 1 shows the electron phase space plots  $(x, \gamma)$  and the profile of  $\bar{B}_z(x)$  at  $\omega_{pe}t = 4500$ . The color indicates the number density  $n$  in the  $(x, \gamma)$  plane. In the lower panel, 1Dt electrons are trapped and energized in the main pulse region. However, in the upper panel, energetic 2Ds electrons are distributed over a wide region from downstream to upstream of the shock wave. Some of them are detrapped from the main pulse after being energized in the pulse. The maximum  $\gamma$  of the 2Ds electrons is higher than that of the 1Dt electrons.

Figure 2 shows typical orbits for two 2Ds electrons. Both electrons are trapped in the main pulse and then escape from it to the upstream region retaining their high energies. The particle shown in Fig. 2 (a) is detrapped at  $\omega_{pe}t \approx 2500$ . It then reenters the shock wave as a result of its gyromotion and is accelerated to a higher energy by the transverse electric field  $E_y$  in the shock wave; the energy increases once in the gyroperiod. This process was repeated several times, and  $\gamma$  rised stepwise. The particle shown in Fig. 2 (b) also departs from the main pulse at  $\omega_{pe}t \approx 2500$ . However, it does not gain energy after detrapping and moves away from the pulse without reentering it. Compared to electron (a), electron (b) has smaller  $\gamma$  (hence, smaller gyroradius) when it escapes from the main

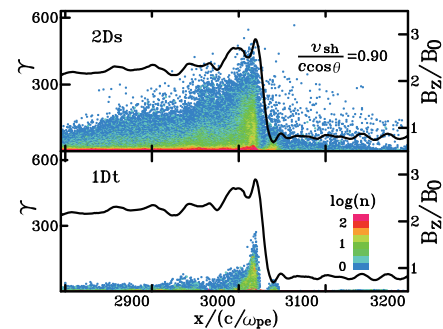


Fig. 1 Phase space plots  $(x, \gamma)$  of 2Ds and 1Dt electrons and profile of 1D magnetic field  $\bar{B}_z(x)$  at  $\omega_{pe}t = 4500$  for the case of  $v_{\text{sh}} = 0.90c \cos \theta$  ( $v_{\text{sh}} = 0.90$ ).

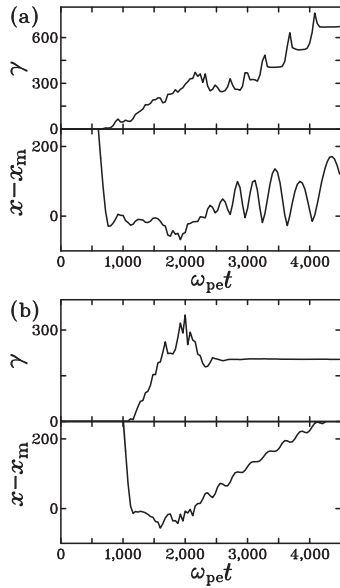


Fig. 2 Orbits of two 2Ds electrons detrapped to the upstream region. Electron (a) suffers the subsequent acceleration, and electron (b) does not.

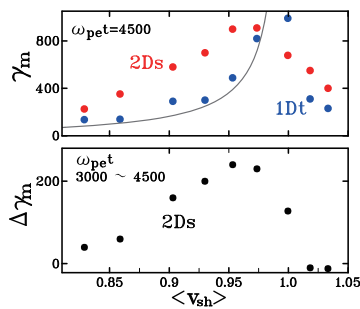


Fig. 3 Maximum  $\gamma$  of 2Ds and 1Dt electrons,  $\gamma_m$ , at  $\omega_{pe}t = 4500$  and increment of  $\gamma_m$  of 2Ds electrons from  $\omega_{pe}t = 3000$  to 4500 as functions of  $\langle v_{sh} \rangle$ .

pulse. As a result, electron (b) does not reenter the shock wave.

In this paper, we do not consider electrons detrapped to the downstream region. Such electrons move backward relative to the main pulse and their  $\gamma$ -values oscillate with the gyroperiod [2];  $\gamma$  decreases when the gyromotion is parallel (antiparallel) to  $E_y$  that is positive in the downstream region. Therefore, the net increase in  $\gamma$  after detraping is almost zero.

We now consider the dependence of electron motions on  $v_{sh}$ . Figure 3 shows maximum values of  $\gamma$ , denoted by  $\gamma_m$ , for 2Ds electrons (red circles) and 1Dt electrons (blue circles) at  $\omega_{pe}t = 4500$  as functions of  $\langle v_{sh} \rangle$  given by Eq. (2). The solid line represents the theory (1), which was derived under the assumption that a shock wave is 1D and stationary. This theory is in good agreement with the  $\gamma_m$ -values of 1Dt electrons for the range of  $\langle v_{sh} \rangle < 1$ . The values of  $\gamma_m$  for 2Ds electrons are greater than those of for

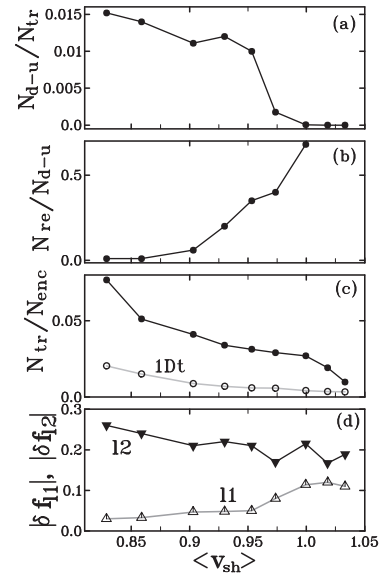


Fig. 4 Numbers of 2Ds electrons (a) detrapped to the upstream region and (b) reentered the shock wave after detraping by  $\omega_{pe}t = 4500$  as functions of  $\langle v_{sh} \rangle$ . (c) The numbers of trapped 1Dt and 2Ds electrons and (d) magnitudes of 1D and 2D fluctuations.

1Dt electrons for all  $\langle v_{sh} \rangle$  except quite close to  $\langle v_{sh} \rangle = 1$ . The 2Ds electrons are accelerated to the highest energies when  $\langle v_{sh} \rangle \approx 0.95$ . The lower panel shows the increment of  $\gamma_m$ ,  $\Delta\gamma_m$ , of 2Ds electrons from  $\omega_{pe}t = 3000$  to 4500. Some electrons reenter the shock after detraping, which produces  $\Delta\gamma_m$ . The value of  $\Delta\gamma_m$  is greatest at  $\langle v_{sh} \rangle \approx 0.95$ .

Figure 3 is for  $N/10^9 \approx 1.1$ , where  $N$  is the total number of simulation particles. We also performed simulations with  $N/10^9 \approx 0.55$  and 2.2 and obtained essentially the same results for maximum  $\gamma$ -values, although the phase space plots in the  $(x, \gamma)$  plane shown in Fig. 1 are quite discrete in larger  $\gamma$  regions. This indicates that  $N/10^9 \approx 1.1$  is large enough for us to compare the maximum  $\gamma$ -values observed in the simulations with the theory (1).

Figure 4 (a) shows the number of electrons that are detrapped to the upstream region by  $\omega_{pe}t = 4500$ ,  $N_{d-u}$ , as a function of  $\langle v_{sh} \rangle$ . In the figure,  $N_{d-u}$  is normalized to the number of electrons that were trapped in the main pulse by that time,  $N_{tr}$ . When  $\langle v_{sh} \rangle > 1$ , there are no electrons detrapped to the upstream region. As  $\langle v_{sh} \rangle$  decreases from unity,  $N_{d-u}/N_{tr}$  increases. Figure 4 (b) shows the number of electrons that reenter the shock wave after detraping to the upstream region and are then accelerated to higher energies,  $N_{re}$ . Here,  $N_{re}$  is normalized to  $N_{d-u}$  and the values for  $\langle v_{sh} \rangle > 1$  are not plotted. The ratio  $N_{re}/N_{d-u}$  decreases as  $\langle v_{sh} \rangle$  decreases from unity. Figure 4 (c) shows  $N_{tr}$  for 2Ds electrons (black line) and 1Dt electrons (gray line) normalized to the number of electrons that encountered the shock wave  $N_{enc}$ . This indicates that electron trapping is enhanced by 2D fluctuations [3]. As shown in Fig. 4 (d), the amplitudes of 2D fluctuations  $|\delta f_{i2}|$  (black

line) are greater than those of 1D fluctuations  $|\delta f_{11}|$  (gray line), where  $\delta f_{11}$  and  $\delta f_{12}$  are defined by Eq. (5) and the values are averaged over the period from  $\omega_{pe}t = 1000$  to 4500.

## 5. $\theta$ Dependence

In this section, we present results for the cases of  $\theta = 46^\circ$  and  $65^\circ$  in addition to  $\theta = 54^\circ$ . Figure 5 shows maximum  $\gamma$  of electrons,  $\gamma_m$ , at  $\omega_{pe}t = 4500$  and the increment of  $\gamma_m$ ,  $\Delta\gamma_m$ , from  $\omega_{pe}t = 3000$  to 4500 as functions of  $\langle v_{sh} \rangle$  for  $\theta = 46^\circ$  (red),  $54^\circ$  (black), and  $64^\circ$  (blue). Figure 6 shows (a)  $N_{d-u}/N_{tr}$ , (b)  $N_{re}/N_{d-u}$ , and (c)  $v_x$  where  $v_x$  is defined by Eq. (4), in which time-averaged values of  $|\delta f_{11}|$  and  $|\delta f_{12}|$  are substituted.

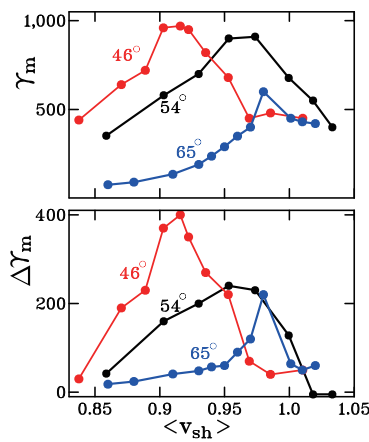


Fig. 5 Maximum  $\gamma$  of 2Ds electrons at  $\omega_{pe}t = 4500$  and its increment from  $\omega_{pe}t = 3000$  for the cases of  $\theta = 46^\circ$  (red),  $54^\circ$  (black), and  $65^\circ$  (blue).

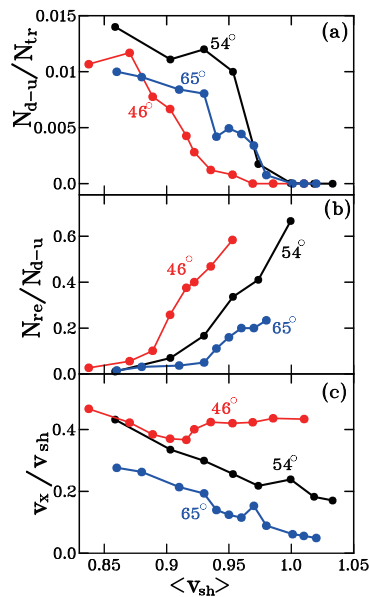


Fig. 6 Numbers of electrons (a) detrapped to the upstream region and (b) then reentered the shock wave by  $\omega_{pe}t = 4500$  for  $\theta = 46^\circ$ ,  $54^\circ$  and  $65^\circ$ . (c)  $v_x$  defined by Eq. (4).

We compare the results shown in Figs. 5 and 6 with the equations in Sec. 2. For the range of  $\langle v_{sh} \rangle < 0.94$ ,  $\gamma_m$ ,  $\Delta\gamma_m$ , and  $N_{re}/N_{d-u}$  increase with decreasing  $\theta$ . This can be explained by eqs. (1) and (8). Equation (1) suggests that if the value of  $\langle v_{sh} \rangle$  is fixed,  $\gamma$ -values of electrons trapped in the main pulse would increase with decreasing  $\theta$ . Hence, for smaller  $\theta$ , electrons could have greater  $\gamma$ -values when they depart from the main pulse. Then, a large fraction of detrapped electrons can reenter the shock wave because of their large gyroradii and can be accelerated to higher energies. According to Eq. (8), the increment in  $\gamma$  due to this process would be enhanced as  $\gamma$  increases. Therefore, we can expect that  $\gamma_m$ ,  $\Delta\gamma_m$ , and  $N_{re}/N_{d-u}$  would increase as  $\theta$  decreases, which is consistent with the results for the range  $\langle v_{sh} \rangle < 0.94$ . However, for the range of  $\langle v_{sh} \rangle > 0.94$ , the simulation results are not consistent with the above equations;  $\gamma_m$ -values for  $\theta = 46^\circ$  are smaller than those for  $\theta = 54^\circ$ . Figure 6 (a) shows that electron detrapping to the upstream region does not occur ( $N_{d-u}/N_{tr} \approx 0$ ) for  $\theta = 46^\circ$  and  $\langle v_{sh} \rangle > 0.96$ . As described in Sec. 2, it can be expected that detrapping would be enhanced as  $v_x$  increases. This is consistent with the results for  $\theta = 54^\circ$  and  $64^\circ$ ; both  $N_{d-u}/N_{tr}$  and  $v_x$  increase as  $\langle v_{sh} \rangle$  decreases from unity. However, this is inconsistent with the results for  $\theta = 46^\circ$  and  $\langle v_{sh} \rangle > 0.96$ ; although the  $v_x$ -values are not small,  $N_{d-u} \approx 0$ . We have not yet understood the reason for this discrepancy and need further investigation.

## 6. Summary and Discussion

We use a 2D relativistic electromagnetic particle code with full ion and electron dynamics to study electron motions in an oblique shock wave; the study includes trapping in the main pulse, detrapping from the pulse to the upstream region, and subsequent acceleration as a result of gyromotion. We performed simulations for the cases of various values of  $v_{sh}$  and  $\theta = 46^\circ$ ,  $54^\circ$ , and  $65^\circ$ . If  $\theta$  is fixed, the electron  $\gamma$  becomes maximum at  $v_{sh}$  slightly smaller than  $c \cos \theta$ . If the value of  $v_{sh}/(c \cos \theta)$  is fixed,  $\gamma$  tends to increase as  $\theta$  decreases, for the range  $v_{sh}/(c \cos \theta) < 0.94$ . We examined the number of accelerated electrons.

In this paper, we set  $|\Omega_e|/\omega_{pe} = 5$  and  $m_i/m_e = 400$ . These parameters can influence the structure of a shock wave and electron motions in it. The Alfvén Mach number of a shock wave with  $v_{sh} \approx c \cos \theta$  is written as

$$M_A \approx (m_i/m_e)^{1/2} (\omega_{pe}/|\Omega_e|) \cos \theta. \quad (9)$$

As shown in Fig. 6, the electron detrapping to the upstream region was suppressed when  $\langle v_{sh} \rangle > 0.95$  and  $\theta = 46^\circ$ , for which  $M_A > 3$ . When  $|\Omega_e|/\omega_{pe} = 6$ ,  $M_A$  is reduced to 2.3 for  $\theta = 45^\circ$  and  $\langle v_{sh} \rangle \approx 0.95$ . The 2D simulation for this case clearly demonstrated that electron detrapping to the upstream region and subsequent acceleration occur [7]. (For the case  $|\Omega_e|/\omega_{pe} = 3$ ,  $\theta = 45^\circ$ , and  $m_i/m_e = 100$ , electron detrapping and subsequent acceleration were observed for a wave with  $\langle v_{sh} \rangle = 0.95$  and  $M_A = 2.3$  [2].) For

future work, we intend to investigate the  $M_A$  dependence of electron motions in detail. In addition, it is desirable to confirm electron detrapping and subsequent acceleration using simulations with the real ion-to-electron mass ratio.

### Acknowledgments

This work was carried out as part of the collaboration program under Grant Nos. NIFS12KNSS036 and NIFS12KNXN246 of the National Institute for Fusion Science, and of the joint research program of the Solar-Terrestrial Environment Laboratory, Nagoya University, and was supported in part by a Grant-in-Aid for Scientific

Research (C) Grant No. 24540535 from the Japan Society for the Promotion of Science.

- [1] N. Bessho and Y. Ohsawa, Phys. Plasmas **6**, 3076 (1999).
- [2] K. Shikii and M. Toida, Phys. Plasmas **17**, 082316 (2010).
- [3] M. Toida and J. Joho, J. Phys. Soc. Jpn. **81**, 084502 (2012).
- [4] A. Zindo, Y. Ohsawa, N. Bessho and R. Sydora, Phys. Plasmas **12**, 052321 (2005).
- [5] S. Usami and Y. Ohsawa, Phys. Plasmas **9**, 1069 (2002).
- [6] N. Bessho and Y. Ohsawa, Phys. Plasmas **9**, 979 (2002).
- [7] M. Toida and J. Joho, Plasma Fusion Res. **8**, 2401031 (2013).